

Assessing Estrogen Receptors' Status by Texture Analysis of Breast Tissue Specimens and Pattern Recognition Methods

Spiros Kostopoulos¹, Dionisis Cavouras², Antonis Daskalakis¹, Ioannis Kalatzis²,
Panagiotis Bougioukos¹, George Kagadis¹, Panagiota Ravazoula³,
and George Nikiforidis¹

¹ Medical Image Processing and Analysis Group, Laboratory of Medical Physics, School of Medicine, University of Patras, 26500, Rio, Greece

² Medical Image and Signal Processing Laboratory, Department of Medical Instruments Technology, Technological Educational Institute of Athens, 12210 Athens, Greece

³ Department of Pathology, University Hospital of Patras, 26500 Rio, Greece
{skostopoulos, daskalak}@upatras.gr,

{cavouras, ikalatzis}@teiath.gr, {kagadis, gnikif}@med.upatras.gr

Abstract. An image analysis system (IAS) was developed for the quantitative assessment of estrogen receptor's (ER) positive status from breast tissue microscopy images. Twenty-four cases of breast cancer biopsies, immunohistochemically (IHC) stained for ER, were microscopically assessed by a histopathologist, following a clinical routine scoring protocol. Digitized microscopy views of the specimens were used in the IAS's design. IAS comprised a/image segmentation, for nuclei determination, b/extraction of textural features, by processing of nuclei-images utilizing the Laws and Gabor filters and by calculating textural features from the processed nuclei-images, and c/PNN and SVM classifiers design, for discriminating positively stained nuclei. The proportion of the latter in each case's images was compared against the physician's score. Using Spearman's rank correlation, high correlation was found between the histopathologist's and IAS's scores ($\rho=0.89$, $p<0.001$) and 22/24 cases were correctly characterised, indicating IAS's reliability in the quantitative evaluation of ER as additional assistance to physician's assessment.

Keywords: Image Analysis; Pattern Recognition; Estrogen Receptor; Breast Cancer; Histopathology.

1 Introduction

Estrogens receptor (ER) and progesterone receptors are important because their protein levels are raised in pre-malignant and malignant breast lesions [1]. ERs have been used in prognosis [2] and their positive status is of clinical value in adjuvant hormonal therapy of patients with breast carcinomas [3]. Recently, evaluation of the ER-status is performed by means of immunohistochemistry (IHC) [4, 5]. In daily clinical practice, estimation of the ER's status is based on the subjective evaluation of the expressed nuclei in each

specimen, through visual inspection under light microscope. To objectify the ER's status, previous studies have introduced computer-based image analysis approaches [5].

Previous work, concerning quantitative determination of the ER-status, is mainly confined to the utilization of commercially developed image analysis systems, that make use of global thresholding techniques [6-9] to identify positively expressed pixels, and to in-build systems, that employ colour-space transformations together with either unsupervised (clustering by K-means) [10] or supervised classification (multi-layer feed-forward neural network) [11], to specify the number of expressed nuclei.

In this work, a texture based image analysis system (IAS) is proposed for the quantitative assessment of estrogen receptor's (ER) positive status from breast tissue microscopy images. IAS comprised nuclei segmentation, utilizing the recently introduced frequency histogram of connected elements (FHCE) [12], and pattern recognition algorithms (support vector machine (SVM) and probabilistic neural network (PNN)), trained by textural features, to identify positively stained nuclei, for subsequent ER-status determination. The contribution of the present study is the proposal of textural features, related to the texture of ER-expressed nuclei that might be of clinical importance, and the application of state-of-art pattern recognition methods to identify with high precision the ER-status of breast carcinomas.

2 Material and Methods

2.1 Data Collection and Manual Assessment

Clinical material comprised twenty-four breast cancer biopsies, collected from the University Hospital of Patras, Greece. Biopsy's specimens were stained by IHC and were assessed by an experienced histopathologist (P.R) for ER positive status, based on a clinical scoring protocol that follows the recommendations of the American Society of Clinical Oncology [6]. The routine protocol accounts for the percentage of the number of positively stained nuclei (brown) to the total number of nuclei in the case (brown and blue). The scoring scale coded 0 for the range 0–5% and 1, 2, 3, 4 for the ranges 6–10%, 11–33%, 34–66%, 67–100%, respectively. The studied cases had a physician's percentage positivity range between 20%–90% (2–4 scores).

For each specimen, a representative region was specified by the histopathologist. Microscopic specimens were digitized (1300x1030x48bit) at a magnification of x400, using a light microscopy imaging system consisting of a Zeiss Axiostar-Plus microscope and a Leica DC300F colour video camera.

2.2 Image Segmentation and Feature Extraction

For segmentation of nuclei, images were converted to greyscale (1300x1030x8bit) and the Frequency Histogram of Connected Elements (FHCE), proposed by Patricio and Maravall [12], was used. FHCE takes into consideration the spatial properties of the image and embodies the concepts of *connectivity level* and *morphological component* respectively. FHCE is defined as [12]:

$$H(T) = \sum_{\forall (i,j) \in I} C_{i,j}(T) \quad 0 \leq T \leq I_{\max} - 1 \quad (1)$$

where, I_{\max} is the maximum greyscale level of the image $I_{(i,j)}$, $C_{i,j}(T) \in [T - \varepsilon, T + \varepsilon]$ is the connected element, ε is the connectivity level, and T is the grey level. The morphological component, used in the present study, was the four-neighbourhood operator (cross shape). While the image was scanned by the component, a decision was taken whether it constituted a connected element, according to Eq.1. The grey-value of the central pixel was used to form the frequency histogram of the connected components. Upon this bimodal histogram, a threshold was determined to convert the original image into a binary segmented image, with white pixels corresponding to nuclei and black pixels to background.

The resulted image was further processed by morphological (closing followed by opening) and size filters (objects of more than 300 pixels were considered as nucleus), to eliminate small and noisy regions, and fill holes operations to account for original nuclei shape (Fig. 2 left). The expert concluded on the success of nuclei detection in terms of correct and wrongly segmented nuclei, by evaluating the segmented nuclei on three specimens. On average 88.7% of nuclei were correctly identified. The misidentification ratio was of limited significance, since it accounted for both positively and non-positively expressed nuclei and the number of segmented nuclei was considered by the histopathologist adequate for the specimen.

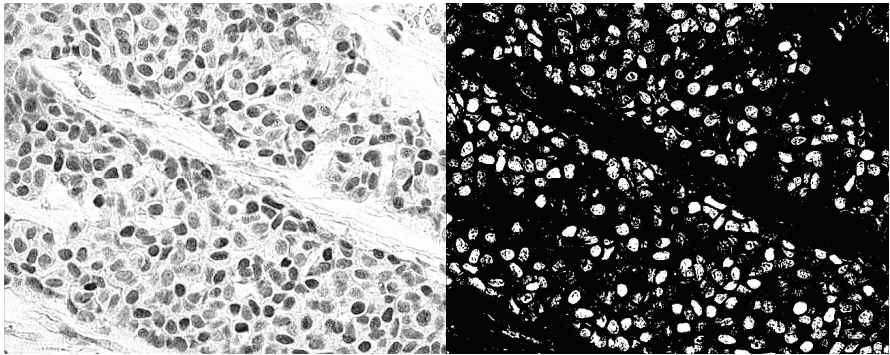


Fig. 1. Left: The original greyscale image, Right: Final segmented image by the FHCE method

Each original greyscale-image was convolved by the Laws' masks [13], thus resulting in 25 processed images. Consequently, all images were transformed to texture energy images (TEM), by measuring local texture energy as the average of absolute values of a 15x15 window. Images were finally reduced to 15 (E5L5, S5L5, W5L5, R5L5, S5E5, W5E5, R5E5, W5S5, R5S5, R5W5, E5E5, S5S5, W5W5, R5R5, L5L5) by suitably combining images to produce rotational invariant images. Kernels initials are accounting for Level, Edge, Spot, Wave, and Ripple detection while the number denotes the size of the mask. These masks are derived by convolving the three basic vectors $L3 = (1, 2, 1)$, $E3 = (-1, 0, 1)$ and $S3 = (-1, 2, -1)$ with each other. Those three

vectors represent smoothed local averaging, symmetric first differencing for edge detection and second differencing for spot detection respectively.

Sixteen sets of 38 textural features were generated from each nucleus, one set from the original greyscale image and 15 from the TEM images. Extracted textural features, encoded chromatin arrangement and ER content, comprised four features from the nucleus's histogram [14], 24 from the grey level spatial-dependence (GLSD) matrix [15], and 10 from the run-length (RL) matrix [16].

In addition, segmented nuclei were also processed by a bank of Gabor filters [17], for comparative evaluation purposes. The impulse response of the Gabor's filters is given by

$$G(x, y) = \exp\left\{-\frac{1}{2}\left[\frac{x^2}{\sigma_x^2} + \frac{y^2}{\sigma_y^2}\right]\right\} \cos(2\pi xf + \phi) \quad (2)$$

where σ_x , σ_y are space constants, f is the radial frequency of the filter and ϕ stands for symmetric (0) and antisymmetric ($-\pi/2$) kernels. In the present study, 10 Gabor filters of size 5×5 were used accounting for 0, 2, 4, 6, 8 and 16 multiplicities of the fundamental frequency and two orientations of $\pi/4$ and $3\pi/4$. Segmented nuclei were convolved with each one of the filters resulting in Gabor energy nuclei images. From each Gabor energy nuclei image, two Gabor texture energy (GTE) features, the mean value and the standard deviation, were calculated [17], thus, constituting a set of 20 GTE features.

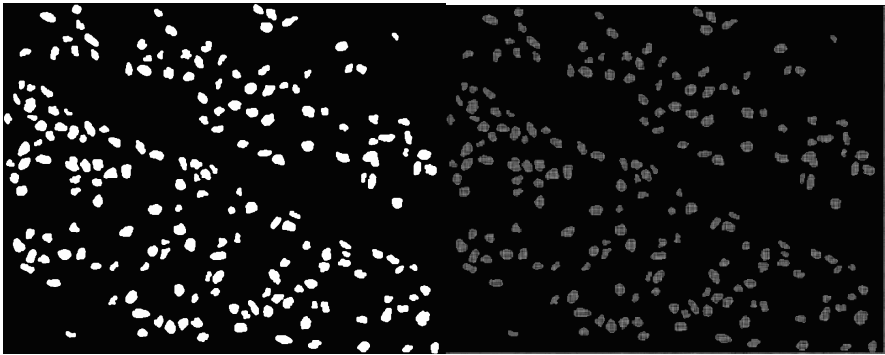


Fig. 2. Left: Final segmented image after the application of morphological, size filters, and fill holes operations, Right: The segmented nuclei superimposed (logical AND operation) onto the R5L5 Laws' TEM image

2.3 Nuclei Classification

The PNN [18] and SVM [19] classifiers were used for the discrimination between brown and blue nuclei, with discriminant functions given by (Eq. 3) and (Eq. 4) respectively:

$$d_i(x) = \frac{1}{(2\pi)^{d/2} \sigma^d} \frac{1}{N} \sum_{k=1}^N \exp \left[-\frac{(x - x_{ik})^T (x - x_{ik})}{2\sigma^2} \right] \quad (3)$$

$$g(x) = \text{sign} \left(\sum_{i=1}^N a_i y_i \cdot [x \cdot x_{ik} (1 + x \cdot x_{ik})] + b \right) \quad (4)$$

where sigma σ is the smoothing factor (experimentally determined to be 0.27), N is the number of nuclei/patterns forming the class i , d is the dimensionality of feature vector, x_{ik} is the k^{th} nucleus/pattern of class i , a_i, b are weight coefficients, and x is the unknown feature vector. In the present study we used the Quadratic kernel. The optimization problem was solved by using the least squares function provided with MATLAB optimization toolbox.

Optimum classifier design was accomplished via its performance evaluation. This involved selection of the best feature combination, using the exhaustive search algorithm (forming feature patterns sets in all possible combinations of 2, 3, 4, and 5 features) and the leave-one-out method [14], employing as training data a set of brown and blue nuclei, selected by the histopathologist on the RGB digitized images of 3 biopsy specimens. The aim was to determine that feature set that provided highest discrimination accuracy with the least number of features. Features were previously normalized to zero mean value and unit variance [14], according to $\tilde{x}_i = (x_i - \mu) / \text{std}$, where x_i and \tilde{x}_i are features prior to and after normalization, μ and std are the mean value and standard deviation of each feature respectively, taking into account all members of both classes (positively and non-positively stained nuclei, specified as training data by the physician).

2.4 Computer-Aided Assessment of ER-Status

Following classifier design, the proposed IAS system assessed the ER positivity status of each case by automatically detecting the number of positively (brown) and non-positively (blue) stained nuclei from the greyscale digitized images of the specimen, based solely on nuclei textural information, and by forming the ratio of positive to positive and non-positive nuclei. That ratio was referred to the scoring scale (see section 2.1).

3 Results

For classifier design purposes, the histopathologist randomly specified 270 "brown" and 111 "blue" nuclei out of three cases. These nuclei constituted the 'gold standard' for the design of the PNN classifier. Table 1 presents the PNN's performance in terms of overall accuracy for different feature-combinations, for the original grey-scale image, the 15 images processed by Law's kernels and for the GTE features. Additionally, the comparable performance of SVM is shown. Table 2 shows the IAS's performance in assigning ER-status to specimens against the histopathologists' estimation.

Table 1. Classifier's performance in discriminating brown from blue nuclei in the original and processed by Law's and Gabor's kernels images

images	PNN's accuracy per feature combination (%)			
	2	3	4	5
Original	84.47	86.16	86.83	83.43
E5L5 ^{Ra}	67.72	71.39	71.13	76.25
S5L5 ^{Ra}	67.98	71.39	72.44	71.25
W5L5 ^{Ra}	68.24	66.40	66.40	68.75
R5L5 ^{Ra}	82.15	84.25	88.51	71.25
S5E5 ^{Ra}	61.42	60.63	64.56	66.25
W5E5 ^{Ra}	62.99	66.40	66.14	66.42
R5E5 ^{Ra}	72.97	74.02	75.07	70.71
W5S5 ^{Ra}	63.51	66.93	68.76	65
R5S5 ^{Ra}	62.20	63.78	64.30	64.27
S5S5 ^{Ra}	65.88	65.62	65.61	62.86
E5E5 ^{Rb}	65.61	66.14	66.40	67.86
S5S5 ^{Rb}	67.19	67.19	68.77	69.29
W5W5 ^{Rb}	62.99	64.57	66.40	63.57
R5R5 ^{Rb}	64.04	63.26	63.25	63.57
L5L5 ^{Rb}	79.26	82.68	83.98	73.57
GTE	89.24	89.76	90.03	90.56
	SVM's accuracy per feature combination (%)			
GTE	89.50	92.12	92.91	94.23

R: rotational invariance
a: TEM images combined for directionality, i.e E5L5^a=E5L5+L5E5
b: consistent TEM with respect to size, ie S5S5^b=S5S5x2

Table 2. Results of the percentage ER positive status evaluation

Physician's ER Score	Computer-aided score			Accuracy
	2	3	4	
2	5	0	0	100%
3	0	6	1	85.7%
4	0	1	11	91.7%
Overall accuracy				91.6%

4 Discussion and Conclusion

In clinical routine practice, ER-status estimation is performed by manually counting and/or visually estimating at a "high power field" (or regions with high concentration of positive nuclei) the percentage of positively stained nuclei to the total number of nuclei in the specimen. In the present study, an image analysis system, based on nuclei textural features and pattern recognition methods, is proposed for the assessment of ER positive status in breast tissue carcinomas. The nuclei were segmented using the FHCE approach. Fig.2 shows an example of the segmentation procedure after the application of morphological and size filters. A series of closing and opening filters,

in association with fill holes operations, were applied after FHCE algorithm to dispose of noisy structures and to complete the nuclei shape (see Fig. 2 left).

Texture analysis has been extensively used in computer-based image analysis in medical research. Here, texture is figured as the interrelationship of the spatial settlement of the pixels, which constitute the nucleus, and as pixel's local power spectrum. The highest discrimination accuracy of the PNN classifier, regarding textural features derived from nuclei on the original image, was 86.3%. The feature combination with the maximum discriminatory power was the mean value, entropy, sum average and grey level non-uniformity. By applying the Laws' kernels in the original image, various structural properties of nuclei texture were emphasized that improved the PNN's classification accuracy to 88.5%. Best textural features were extracted from the R5L5^R image, in which the ripple content of the nuclei-images was emphasised, and comprised the standard deviation, kurtosis, entropy, and run length non-uniformity. The entropy feature, which was found in both feature sets of the original and processed images, is a measure of randomness of greylevel distribution and seems to play an important role in the discrimination of positive from non-positive nuclei. Furthermore, as results indicated, Gabor's textural features facilitate discrimination of stained (expressed) and unstained nuclei resulting in 90.6% and 94.23% overall accuracies for the PNN and SVM classifiers respectively.

The IAS's performance, in assigning an ER-score to each specimen of the study, was compared against a corresponding evaluation by histopathologist. The overall classification agreement was 91.6%, with the IAS system having similarly assigned 22/24 specimens as the histopathologist, while agreement at distinct ER-levels was 100%, 85.7%, and 91.7% for 2,3,4 ER-levels respectively. The Spearman's correlation test revealed high correlation among the histopathologist and the computer-based assessments ($\rho=0.89$, $p<0.001$).

A variety of image analysis methods (commercially available packages and in build algorithms) have been proposed for the quantification of IHC-stained sections [6-10]. Only Schnorrenberg et al [11] have used different scoring protocol and pattern recognition techniques, based on a colour-transformation technique and a multilayer neural network, and they have found a significant correlation in ER-status between manually and image analysis assessment, reporting 84% agreement of their system against the expert's. In comparison, employment by the present study of state-of-art pattern recognition methods and features, related to nuclei's texture, improved (91.6%) the classification of breast carcinomas' ER-status.

In conclusion, employing texture analysis methods to quantitatively evaluate IHC stained breast biopsies could be of value, as an additional tool, to the histopathologist in assessing the ER-status.

Acknowledgments. The first author was supported by a grant from the Greek State Scholarships Foundation (IKY).

References

1. Sommer, S., Fuqua, S.A.: Estrogen receptor and breast cancer. *Semin Cancer Biol.* 11, 339–352 (2001)
2. Donegan, W.L.: Tumor-related prognostic factors for breast cancer. *CA Cancer J. Clin.* 47, 28–51 (1997)

3. Jasani, B., Douglas-Jones, A., Rhodes, A., Wozniak, S., Barrett-Lee, P.J., Gee, J., Nicholson, R.: Measurement of estrogen receptor status by immunocytochemistry in paraffin wax sections. *Methods Mol. Med.* 120, 127–146 (2006)
4. Harvey, J.M., Clark, G.M., Osborne, C.K., Allred, D.C.: Estrogen receptor status by immunohistochemistry is superior to the ligand-binding assay for predicting response to adjuvant endocrine therapy in breast cancer. *J. Clin. Oncol.* 17, 1474–1481 (1999)
5. Diaz, L.K., Sneige, N.: Estrogen receptor analysis for breast cancer: Current issues and keys to increasing testing accuracy. *Adv. Anat. Pathol.* 12, 10–19 (2005)
6. Diaz, L.K., Sahin, A., Sneige, N.: Interobserver agreement for estrogen receptor immunohistochemical analysis in breast cancer: A comparison of manual and computer-assisted scoring methods. *Ann. Diagn. Pathol.* 8, 23–27 (2004)
7. Mofidi, R., Walsh, R., Ridgway, P.F., Crotty, T., McDermott, E.W., Keaveny, T.V., Duffy, M.J., Hill, A.D., O'Higgins, N.: Objective measurement of breast cancer oestrogen receptor status through digital image analysis. *Eur. J. Surg. Oncol.* 29, 20–24 (2003)
8. Lehr, H.A., Mankoff, D.A., Corwin, D., Santeusano, G., Gown, A.M.: Application of photoshop-based image analysis to quantification of hormone receptor expression in breast cancer. *J. Histochem. Cytochem.* 45, 1559–1565 (1997)
9. Makkink-Nombrado, S.V., Baak, J.P., Schuurmans, L., Theeuwes, J.W., van der Aa, T.: Quantitative immunohistochemistry using the cas 200/486 image analysis system in invasive breast carcinoma: A reproducibility study. *Anal. Cell Pathol.* 8, 227–245 (1995)
10. Kostopoulos, S., Cavouras, D., Daskalakis, A., Ravazoula, P., Nikiforidis, G.: Image analysis system for assessing the estrogen receptor's positive status in breast tissue carcinomas. In: *Proceedings of the International Special Topic Conference on Information Technology in Biomedicine, Ioannina Greece (2006)*
11. Schnorrenberg, F., Tsapatoulis, N., Pattichis, C.S., Schizas, C.N., Kollias, S., Vassiliou, M., Adamou, A., Kyriacou, K.: Improved detection of breast cancer nuclei using modular neural networks. *IEEE Eng. Med. Biol. Mag.* 19, 48–63 (2000)
12. Patricio, M.A., Maravall, D.: A comparative study of contextual segmentation methods for digital angiogram analysis. *Cybernetics and Systems: An International Journal* 35, 63–83 (2004)
13. Laws, K.: Rapid texture identification. *Proceedings of the Image Processing for Missile Guidance*, pp. 376–380 (1980)
14. Theodoridis, S., Koutroumbas, K.: *Pattern recognition*, 2nd edn. Elsevier, San Diego (2003)
15. Haralick, R.M., Shanmugam, K., Dinstein, I.H.: Textural features for image classification. *IEEE Trans. Sys. Man. Cyb.* 3, 610–621 (1973)
16. Galloway, M.M.: Texture analysis using gray-level run lengths. *Computer Graphics and Image Processing*. 4, 172–179 (1975)
17. Grigorescu, S.E., Petkov, N., Kruizinga, P.: Comparison of texture features based on gabor filters. *IEEE Trans. Image Processing*. 11 (2002)
18. Specht, D.F.: Probabilistic neural networks. *Neural Networks*. 3, 109–118 (1990)
19. Christanini, N., Taylor, J.S.: *An introduction to support vector machines and other kernel-based learning methods*. Cambridge University Press, Cambridge (2000)